The Plant Cell, Vol. 12, 405–417, March 2000, www.plantcell.org © 2000 American Society of Plant Physiologists

Deficiency in Fatty Acid Synthase Leads to Premature Cell Death and Dramatic Alterations in Plant Morphology

Zhonglin Mou, Yikun He,[1] Ya Dai, Xinfang Liu, and Jiayang Li[2]

Institute of Genetics, Chinese Academy of Sciences, Beijing 100101, China

An Arabidopsis *mosaic death1* (*mod1*) mutant, which has premature cell death in multiple organs, was isolated. *mod1* plants display multiple morphological phenotypes, including chlorotic and curly leaves, distorted siliques, premature senescence of primary inflorescences, reduced fertility, and semidwarfism. The phenotype of the *mod1* mutant results from a single nuclear recessive mutation, and the *MOD1* gene was isolated by using a map-based cloning approach. The *MOD1* gene encodes an enoyl-acyl carrier protein (ACP) reductase, which is a subunit of the fatty acid synthase complex that catalyzes de novo synthesis of fatty acids. An amino acid substitution in the enoyl-ACP reductase of the *mod1* mutant causes a marked decrease in its enzymatic activity, impairing fatty acid biosynthesis and decreasing the amount of total lipids in *mod1* plants. These results demonstrate that a deficiency in fatty acid biosynthesis has pleiotropic effects on plant growth and development and causes premature cell death.

INTRODUCTION

Cell death has been classified into physiological cell death and nonphysiological cell death (Vaux and Korsmeyer, 1999). The former refers to a process programmed by the organism for the purpose of killing its own cells, including apoptosis, aging, terminal differentiation, and defense against pathogen infection. The latter includes cell death from injury caused by external events, such as poisons or lack of nutrients, or from intrinsic defects, such as a mutation in an essential enzyme or expression of an altered gene product that is toxic to the cells.

In plants, two types of physiological cell death have received considerable attention in recent years. One is developmentally programmed cell death (PCD), which includes the degeneration of suspensor and aleurone cells (Yeung and Meinke, 1993), the development of xylem tracheary elements (Fukuda, 1997), and the execution of senescence (Bleecker and Patterson, 1997). The other is the hypersensitive response (HR), which results in cell death at the site of infection by an avirulent pathogen. The HR produces dry lesions that are clearly delimited from the surrounding healthy tissues (Dangl et al., 1996). A large number of mutants characterized by the spontaneous lesion phenotype, which mimics the HR defense responses, have been identified in maize (Gray et al., 1997), barley (Wolter et al., 1993), rice (Marchetti et al., 1983), and Arabidopsis (Dietrich et al., 1994; Greenberg et al., 1994). Because the lesions form in the absence of pathogen infection, these mutants have been collectively called the lesion mimic mutants. In Arabidopsis, the lesion-stimulating disease mutant *lsd1* has been well characterized. LSD1, a zinc finger protein, has been proposed to function as a negative regulator of plant PCD in response to signals emanating from the cells undergoing pathogen-induced HR-mediated cell death (Dietrich et al., 1997).

Blockage of metabolic processes also induces cell death in plants. For example, the maize lesion mimic mutant *Les22* produces minute necrotic spots on leaves, which resemble those triggered during HR in response to pathogens (Hu et al., 1998). This phenotype reflects the accumulation of uroporphyrin, the result of an impairment in the porphyrin biosynthetic pathway. Moreover, in transgenic tobacco plants, overexpression of the transcription factor AmMYB308 inhibits phenolic acid metabolism, which leads to precocious cell death in mature leaves. Here, the cell death exhibits some characteristics of apoptosis, such as condensed nuclei, expanded chloroplasts, and DNA fragmentation (Tamagnone et al., 1998).

Compared with the porphyrin and phenolic acid biosynthetic pathways, the metabolic pathway of fatty acid biosynthesis is more complicated, playing a fundamental role in

[1] Current address: Biology Department, Capital Normal University, Beijing 100037, China.

[2] To whom correspondence should be addressed at Institute of Genetics, Chinese Academy of Sciences, Building 917, Datun Rd., Chaoyang District, Beijing 100101, China. E-mail jyli@igtp.ac.cn; fax 86-10-64873428.

synthesis of basic cellular constituents such as phospholipids and glycerolipids (Somerville and Browse, 1991). Currently, phospholipids and glycerolipids are well recognized to function not only as essential components of the cell membranes but also as important regulators in cell proliferation, differentiation, secretion, and apoptosis (Okazaki et al., 1998). In addition, fatty acids also serve as precursors of the phytohormone jasmonic acid, which has been found in recent years to be indispensable for normal plant growth, development, and response to injury (Farmer et al., 1998). The de novo biosynthesis of fatty acids is performed by fatty acid synthase (FAS), with acetyl-coA used as the starting unit and manoyl-acyl carrier protein (ACP) as the elongator. Unlike animal FAS, which is a multifunctional protein, plant FAS is an easily dissociable multisubunit complex consisting of multiple monofunctional enzymes, including β-ketoacyl synthetase, 3-ketoacyl-ACP reductase, 3-hydroxyacyl-ACP dehydrase, and enoyl-ACP reductase (ENR) (Ohlrogge and Jaworski, 1997), the primary products of which are palmitic acid (16:0) and stearic acid (18:0). These 16:0 and 18:0 fatty acids subsequently enter multiple lipid metabolic pathways to form various glycerolipids and phospholipids, such as diacylglycerol, triacylglycerol, sphingomyelin, and ceramide; to yield very long chain fatty acids, such as cuticular waxes; or to be converted into phytohormones, such as jasmonic acid (Ohlrogge and Browse, 1995).

Many Arabidopsis mutants that are deficient in the pathway steps after the synthesis of 16:0 fatty acid (e.g., *fad2* through *fad8*) have been isolated and characterized (Somerville and Browse, 1991; Ohlrogge and Browse, 1995). These mutants are invaluable in elucidating the complicated lipid biosynthetic pathways and investigating the roles of fatty acids in plant growth and development. However, little is known about the de novo fatty acid biosynthetic pathway from which the multiple lipid syntheses are branched. Because fatty acids are essential to all living organisms, mutations in FAS genes of the de novo biosynthetic pathway may be lethal. This would explain why no mutants deficient in fatty acid biosynthesis steps before production of the 16:0 fatty acid have been isolated in higher plants or animals (Slabas and Fawcett, 1992; Ohlrogge and Browse, 1995), although such mutants have been reported in bacteria (Egan and Russell, 1973; Turnowsky et al., 1989) and yeast (Roggenkamp et al., 1980).

In this study, we report the isolation and characterization of an Arabidopsis premature cell death mutant *mod1* (for mosaic death) and the map-based cloning of the gene responsible for the phenotype. The *MOD1* gene encodes an ENR, which is a component of FAS, catalyzing the final reaction in the de novo fatty acid biosynthesis cycle. A single amino acid substitution in the ENR in the plant mutant causes a marked decrease in ENR activity, which results in the impairment of de novo fatty acid biosynthesis. Phenotypic and molecular analyses of *mod1* indicate that a deficiency in FAS leads to premature cell death and altered morphology in Arabidopsis plants.

RESULTS

Isolation and Genetic Analysis of the *mod1* Mutant

Approximately 500,000 M_2 plants derived from ethyl methanesulfonate mutagenesis were grown under continuous light at 23°C and screened for the appearance of chlorosis. One mutant with a chlorotic and curly leaf morphology was isolated and designated as *mod1*, based on its mosaic death pattern revealed by trypan blue staining (see below). The mutant was backcrossed to wild-type Columbia (Col-0) three times, and the homozygous *mod1* line was used for in-depth analysis.

After reciprocal crosses were made between the homozygous *mod1* and wild-type Col-0 plants, the phenotype of the *mod1* plants was scored in the F_1 and F_2 generations. All 53 F_1 progeny generated from reciprocal crosses grew and developed in the same way as wild-type plants. In the F_2 generation, the segregation of 853 wild-type plants to 275 mutants fit the expectation for a single locus ($\chi^2 = 0.656$; $P = 0.418$). These results indicate that *mod1* carries a single recessive nuclear mutation.

Morphology of *mod1* Plants

When grown under continuous light at 23°C, the typical morphology of the *mod1* plants included curly leaves, chlorotic patches, early senescence of primary inflorescences, distorted siliques, reduced fertility, and semidwarfism (Figure 1). However, in seedlings with fewer than four leaves, no morphological difference was apparent between mutant and wild-type plants (Figures 1A and 1B). The initial visible abnormality of mutant plants was chlorosis in the midvein of the fifth or sixth emerging leaf and in the shoot meristems (Figures 1C and 1D). As the plants grew, most of the leaf center became chlorotic, and the lamina frequently became curly (Figures 1E, 1F, and 1K to 1N). The mutant inflorescences and flower buds were also chlorotic as they emerged, and the primary inflorescences almost always stopped growing when they were several centimeters high (Figures 1G and 1H). The premature senescence of the primary inflorescence in the mutant induced the growth of axillary buds and eventually led to the stunted semidwarf morphology. The fertility of the mutants was reduced, fewer seeds were set in the distorted siliques (Figures 1I and 1J), and the *mod1* seeds had a shriveled appearance and a lower germination rate than the wild-type seeds (data not shown).

Microscopic Structure of *mod1* Leaves

The phenotype of the *mod1* mutants suggested that certain aspects of normal cell growth might be disrupted during

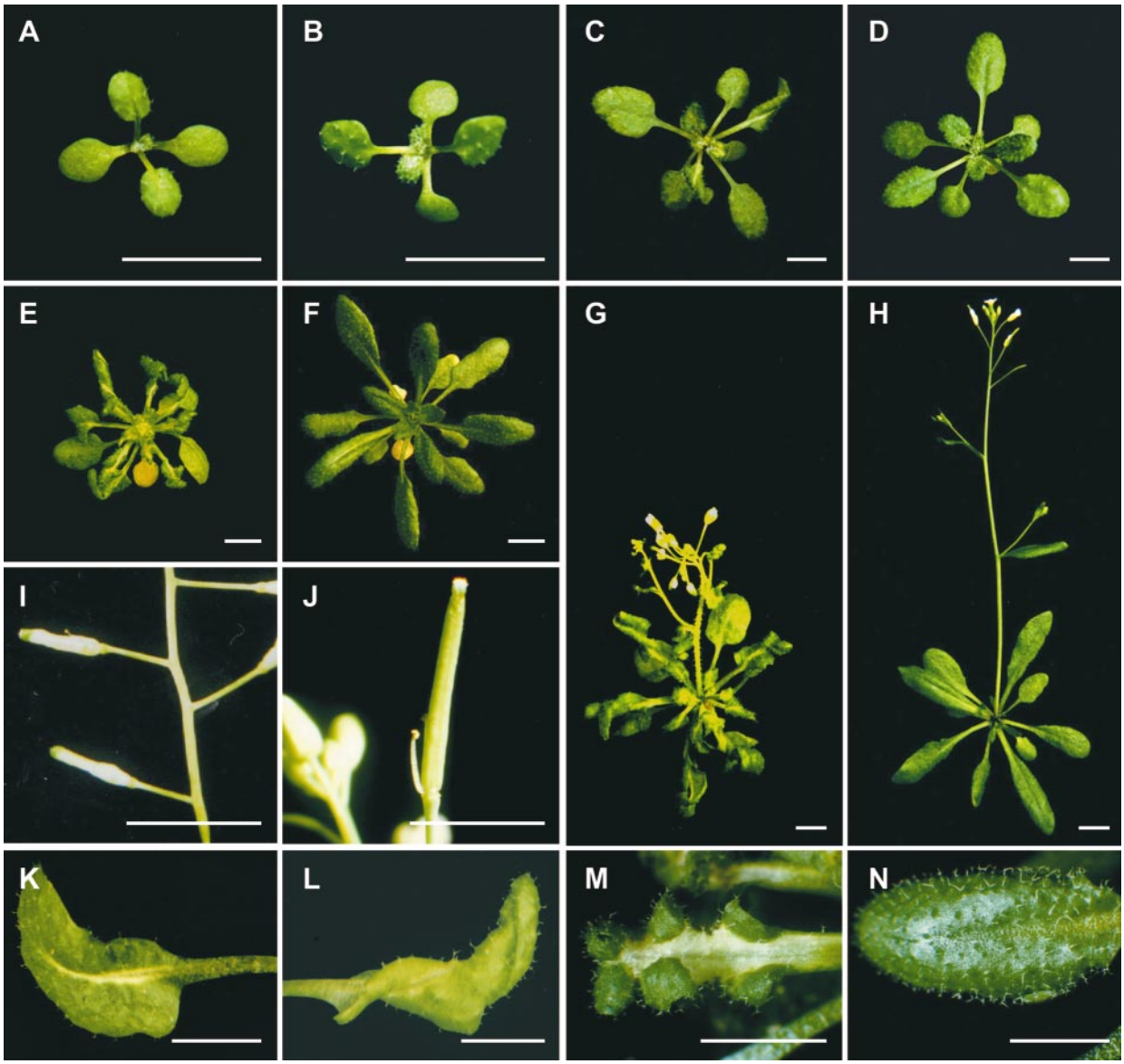

Figure 1. The Phenotype of the *mod1* Mutant.

Wild-type and *mod1* plants were grown under continuous light at 23°C and photographed at the indicated number of days after imbibition.
(A) and **(B)** *mod1* and wild-type plants at day 10.
(C) and **(D)** *mod1* and wild-type plants at day 20.
(E) and **(F)** *mod1* and wild-type plants at day 30.
(G) and **(H)** *mod1* and wild-type plants at day 40.
(I) and **(J)** *mod1* and wild-type siliques.
(K) to **(M)** *mod1* leaves.
(N) Wild-type leaf.
Bars in **(A)** to **(N)** = 0.5 cm.

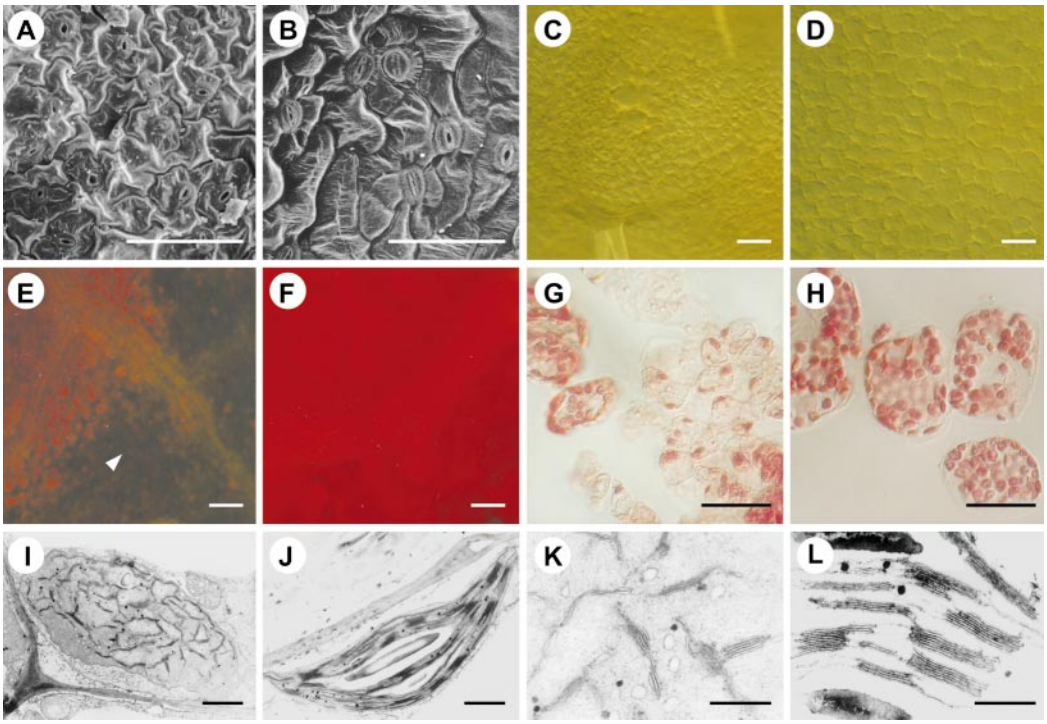

Figure 2. Light and Electron Microscopic Analysis.

(A) and **(B)** Scanning electron microscopy of *mod1* and wild-type epidermal cells.
(C) and **(D)** Differential interference contrast microscopy of *mod1* and wild-type mesophyll cells.
(E) and **(F)** A chlorotic sector (arrowhead) of a *mod1* leaf **(E)** shows much weaker red fluorescence than a wild-type leaf **(F)** under UV light.
(G) and **(H)** *mod1* mesophyll cells **(G)** contain fewer chloroplasts than wild-type cells **(H)**.
(I) and **(J)** Transmission electron microscopy of *mod1* and wild-type chloroplasts.
(K) and **(L)** Transmission electron microscopy of *mod1* and wild-type thylakoid membranes.
Bars in **(A)** to **(H)** = 50 μm; bars in **(I)** and **(J)** = 500 nm; bars in **(K)** and **(L)** = 100 nm.

plant growth and development. To investigate this possibility, we conducted a light and electron microscopic examination of wild-type and *mod1* leaf structures. Compared with the smooth surface of the wild-type leaves, the epidermal cells of *mod1* leaves showed a rumpled surface (Figures 2A and 2B). Moreover, unlike those of the wild type, *mod1* mesophyll cells in and around the chlorotic sectors were irregular in size and shape (Figures 2C, 2D, 2G, and 2H), suggesting that the growth of mesophyll cells was abnormal in *mod1* leaves. However, no irregular cell size or shape was observed in the epidermal or mesophyll cells in the healthy part of the *mod1* leaves (data not shown). The *mod1* mesophyll cells in chlorotic sectors had much weaker red fluorescence under UV light (Figures 2E and 2F).

The latter result prompted us to scrutinize *mod1* chloroplasts. Approximately eight chloroplasts were found in a *mod1* mesophyll cell in the chlorotic area (Figure 2G), a marked reduction from the average of 33 chloroplasts per cell in wild-type plants (Figure 2H). Quantification of the total chlorophyll (*a* and *b*) content of the whole plants revealed a decrease from 1.18 mg per g fresh weight of tissue in the wild type to 0.84 mg per g in the *mod1* mutant. Because only those cells in the chlorotic sectors showed weaker red fluorescence, the decrease in the chlorophyll content in the cells in the chlorotic sectors would be much more significant than that for the whole plant. Probably, the decrease in chloroplast number and chlorophyll content caused the chlorotic phenotype of *mod1* plants. Ultrastructural studies further revealed that in and around the chlorotic sectors, *mod1* grana were not well developed (Figures 2I to 2L). These morphological abnormalities and ultrastructural observations suggest that chloroplast development in *mod1* abnormal leaf sectors was disturbed and that the cells in *mod1* plants may undergo cell death.

Premature Cell Death in the *mod1* Plants

Cell death in *mod1* plants was subsequently demonstrated by staining with trypan blue, a dye that is widely used to

stain dying cells during pathogen-induced PCD (Keogh et al., 1980; Dietrich et al., 1994; Botella et al., 1998; Kamoun et al., 1998; McDowell et al., 1998). When morphologically abnormal *mod1* plants were subjected to trypan blue staining, we found a mosaic pattern of positive staining in leaf mesophyll cells, siliques (Figures 3A to 3D), and roots (data not shown). Under high magnification, single and clustered stained cells were found to have condensed cytoplasm (Figures 3E to 3H), which is reminiscent of animal apoptosis (Wyllie et al., 1980). Furthermore, we conducted several experiments to investigate whether nuclear DNA fragmentation had occurred in *mod1* plants, because DNA fragmentation is one of the characteristics of apoptosis (Bush et al., 1989; Cohen, 1993; Kuo et al., 1996; Wang et al., 1996). DNA gel blot analysis showed an apparent DNA ladder in the total DNA isolated from *mod1* plants (Figure 4, lane 1), whereas this pattern of DNA fragmentation was barely detectable in wild-type plants at an identical developmental stage (Figure 4, lane 2).

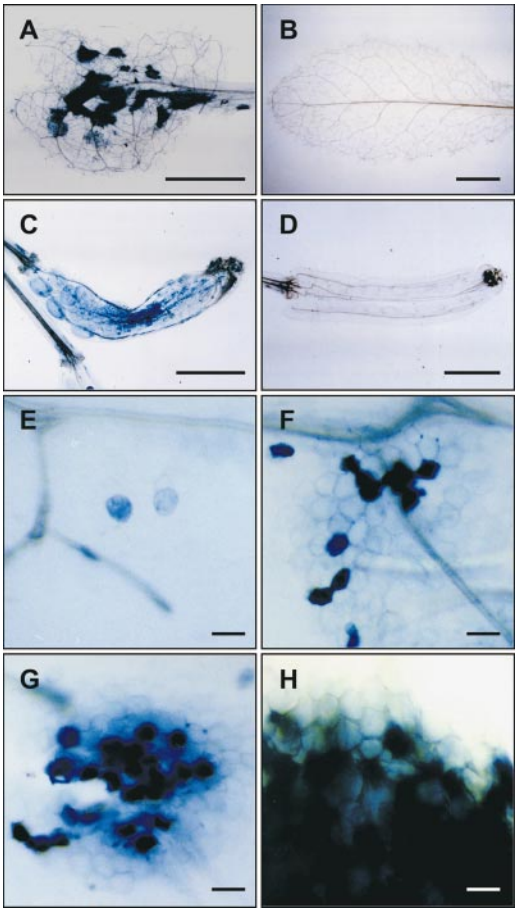

Figure 3. Histochemical Staining with Trypan Blue.

(A) to **(D)** Trypan blue–stained *mod1* and wild-type leaves and siliques, demonstrating a mosaic staining pattern in *mod1* plants (**[A]** and **[C]**).
(E) to **(H)** High magnification of stained single and clustered *mod1* leaf cells.
Bars in **(A)** and **(B)** = 0.25 cm; bars in **(C)** and **(D)** = 0.1 cm; bars in **(E)** to **(H)** = 25 μm.

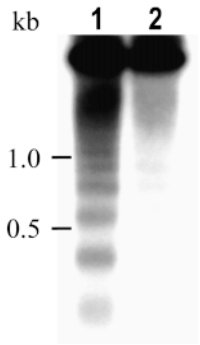

Figure 4. DNA Fragmentation in *mod1* Plants.

The DNA ladder of *mod1* plants was detected by DNA gel blot analysis with a ^{32}P-labeled total DNA digested with Sau3AI. Equal amounts of total DNA isolated from *mod1* and wild-type plants at the same developmental stage were loaded in each lane. Lane 1, DNA isolated from *mod1* plants; lane 2, DNA isolated from wild-type plants. Positions of DNA standards (identified in kilobases) are indicated at left.

mod1 Mutants Are Sensitive to Temperature

To investigate the influence of physiological and environmental factors on the phenotype of *mod1* mutants, we examined the plants under various growth conditions. Although plant nutrients and growth regulators, such as indole-3-acetic acid, cytokinin (kinetin), abscisic acid, and gibberellin (GA_3), had no effect on the phenotype of the *mod1* mutants (data not shown), temperature had a strong influence. When grown under continuous light at an above-normal temperature (26°C), *mod1* plants showed mutant characteristics at the four-leaf stage by day 20 (data not shown) and developed a severe phenotype by day 40 (Figures 5A and 5B). The extreme phenotype included markedly shortened inflorescences and substantially delayed flowering time with reduced fertility. In contrast, *mod1* plants grown at 23°C showed only a moderate semidwarf phenotype and slightly reduced fertility (Figure 1G). When *mod1* plants were grown at an even lower temperature (20°C), the phenotype was even less affected (Figures 5C and 5D).

Map-Based Cloning of the *MOD1* Locus

To map the *MOD1* locus, we crossed the homozygous *mod1* line (Col-0 background) to the polymorphic ecotype

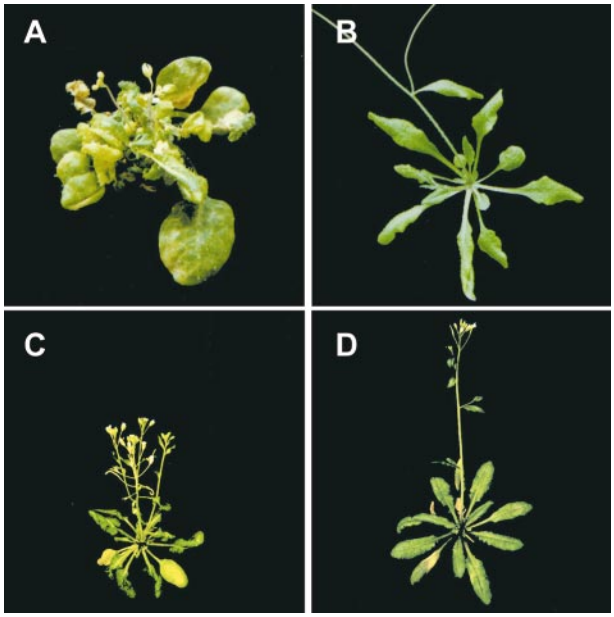

Figure 5. Effect of Temperature on *mod1* Plants.

(A) and **(B)** *mod1* and wild-type plants grown under continuous light at 26°C for 40 days.
(C) and **(D)** *mod1* and wild-type plants grown under continuous light at 20°C for 40 days.

Landsberg *erecta* (L*er*) and self-pollinated the F_1 progeny to yield an F_2 mapping population. Linkage analysis of 822 F_2 plants that showed the *mod1* mutant phenotype placed the *MOD1* locus at the top of chromosome 2, between the molecular markers *IGS1* and mi421 (Figure 6A). The three yeast artificial chromosome (YAC) ends within this interval, CIC9A3R, CIC11C7L, and CIC2G5R, were isolated and tested for polymorphisms between the Col-0 and L*er* genetic backgrounds. CIC9A3R was converted into a cleaved amplified polymorphic sequence (CAPS) marker, mapped, and found to be the closest marker to *MOD1* on the telomeric side of the locus (Figure 6A). To narrow the search for the *MOD1* locus, we hybridized the three YAC ends (CIC9A3R, CIC11C7L, and CIC2G5R) and the restriction fragment length polymorphism marker CDs3 to a bacterial artificial chromosome (BAC) library and identified 31 BAC clones. A contig was constructed, and four new CAPS markers (TAMU6P5-4.8, TAMU18A18E1, TAMU18A18E2 and TAMU12A21E1) were further developed (Figure 6A). Recombination analysis of 2014 F_2 mutants indicated that the *MOD1* locus was located in the interval between TAMU6P5-4.8 and CIC9A3R. DNA gel blot analysis showed that both markers were in the same BAC clone, TAMU6P5 (Figure 6A). Therefore, we screened a λ genomic library, using these two markers as probes, and obtained two overlapping λ clones. Two new CAPS markers, T6P5-14 and T6P5-11, were further derived from these λ DNA fragments, and the *MOD1* locus was further delimited within a 9-kb region (Figure 6A).

We then subcloned and sequenced the 9-kb wild-type Col-0 DNA fragment and compared its sequence with the DNA and protein databases. BLAST analysis identified several DNA sequences encoding ENR in Arabidopsis ecotype L*er* (GenBank accession number Y13860), oilseed rape (GenBank accession number X95462), rice (GenBank accession number AJ003025), and tobacco (GenBank accession number Y13861), in addition to the sequence of BAC clone TAMU6P5 (GenBank accession number AC005970). Annotation of the 9-kb genomic DNA region indicated that it contains a complete *ENR* gene and a partial open reading frame for reverse transcriptase. These results suggested that *MOD1* might encode ENR.

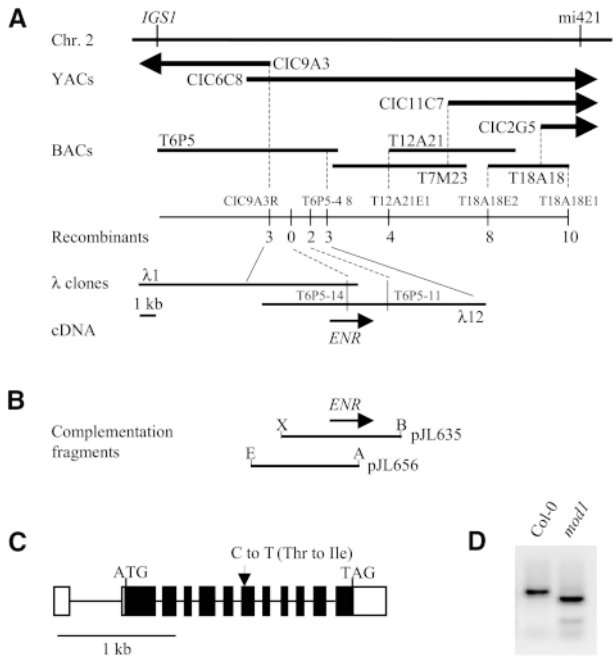

Figure 6. Molecular Identification of the *mod1* Gene.

(A) Physical mapping of the *mod1* locus.
(B) The two DNA fragments used for complementation of the *mod1* mutant. A, AccI; B, BamHI; E, EcoRI; X, XbaI.
(C) Structure of the *ENR* gene and its mutation in the *mod1* plant. The start codon (ATG) and stop codon (TAG) are indicated. The GenBank accession number for *ENR* cDNA (Col-0) is AF207593. Filled boxes denote the coding sequence; open boxes, 5′ and 3′ untranslated regions; lines between boxes, introns.
(D) DNA polymorphism between *mod1* and wild-type plants. The mutation in the *mod1* genomic DNA introduces a new EcoRV site. The DNA fragments flanking the EcoRV site were amplified from the wild-type (Col-0) and *mod1* plants, digested with EcoRV, and separated on an agarose gel.

Confirmation That *MOD1* Encodes ENR by Complementation

To confirm that the *MOD1* locus encodes ENR, we constructed two pBI101-derived binary plasmids, pJL635 and pJL656 (Figure 6B), and transformed mutants with these plasmids by using Agrobacterium (Bechtold et al., 1993). Plasmid pJL635 carries a 7-kb genomic DNA fragment containing the entire *ENR* open reading frame and 4 kb of upstream sequence, whereas plasmid pJL656 carries a 6.5-kb fragment containing a partial *ENR* open reading frame. As summarized in Table 1, all pJL635 T_1 transformants grew and developed in the same way as wild-type plants, whereas none of the pJL656 T_1 transformants showed complementation of the phenotype of the *mod1* mutants. These results indicate that the mutation in *ENR* is responsible for the abnormal morphology of the *mod1* plants. This conclusion was further supported by the segregation ratio of the T_2 progeny from six self-pollinated pJL635 lines (Table 1). Lines 1 to 4 and 6 showed a 3:1 segregation, which is consistent with a single copy of the *MOD1* transgene. Line 5 showed 15:1 segregation, which is consistent with the insertion of two copies of *MOD1* at unlinked loci in this transgenic line.

To find the mutation in the mutant *ENR* gene, we amplified DNA fragments encompassing the gene by polymerase chain reaction from the mutant plants. DNA sequencing revealed a single base substitution of T for C in the mutant *ENR* gene (Figure 6C), a substitution that introduced an EcoRV restriction site into the *mod1* genome. We then used this feature to develop a CAPS marker that would distinguish the mutant from the wild type genotypically (Figure 6D) when analyzing transgenic plants during complementation experiments.

Table 1. Complementation of *mod1* by Transformation

			Phenotype			
Generation	Line	Total[a]	Wild type[b]	Mutant[b]	χ^2	P Value
T_1 (pJL635)		82	82	0		
T_1 (pJL656)		8	0	8		
T_2 (pJL635)	1	50	39	11	0.24[c]	0.62
	2	25	19	6	0.013[c]	0.91
	3	8	6	2	0[c]	1
	4	40	31	9	0.133[c]	0.72
	5	30	28	2	0.009[d]	0.92
	6	21	16	5	0.016[c]	0.90

[a] Total number of transgenic plants analyzed.
[b] Number of plants that showed wild-type or mutant phenotype.
[c] χ^2 values were calculated for a hypothesized 3:1 ratio of wild-type to mutant phenotype for T_2 segregation.
[d] χ^2 values were calculated for a hypothesized 15:1 ratio of wild-type to mutant phenotype for T_2 segregation.

Molecular Properties of the *ENR* Gene in Arabidopsis

DNA gel blot analysis indicates that the Arabidopsis Col-0 ecotype contains only one copy of *ENR* (Figure 7), consistent with the finding in L*er* (Stuitje et al., 1993). Using the *ENR* gene as a probe, we isolated *ENR* cDNAs from an Arabidopsis cDNA library (Col-0). Sequence analysis indicated that the predicted Col-0 ENR protein is virtually identical to that of L*er* (Stuitje et al., 1993), except for two amino acid residues. The *ENR* genes from both the Col-0 and L*er* ecotypes contain one intron in the 5′ untranslated region and 10 introns in the coding region (Figure 6C), and they encode predicted polypeptides of 390 amino acid residues with a calculated molecular mass of 41.3 kD. Moreover, the *ENR* gene of Col-0 contains one abnormal GC splice junction in the seventh intron, as do the corresponding genes in L*er* and rapeseed (Stuitje et al., 1993). As previously observed for other plant ENR proteins (Kater et al., 1991), the Arabidopsis protein possesses a putative plastid transit sequence, an N-terminal extension not present in the corresponding microbial proteins (Bergler et al., 1994). This is consistent with the biochemical finding that in plants, de novo fatty acid biosynthesis occurs in plastids (Ohlrogge and Jaworski, 1997).

The *mod1* Mutation Causes a Marked Decrease in ENR Enzymatic Activity

To understand the effect of the *mod1* mutation on ENR, we compared the amounts of mRNA and protein and the enzymatic activity between wild-type and *mod1* plants. RNA gel blot analysis revealed no substantial differences between wild-type and *mod1* plants (data not shown). Although protein gel blot analysis showed that the amount of ENR protein in *mod1* was ~50% less than that in wild-type plants (Figure 8A), this difference in quantity could not adequately explain the marked difference in enzymatic activity between wild-type and *mod1* mutant plants (Figure 8B). Therefore, we concluded that in *mod1* plants, the C-to-T missense mutation, which in turn encodes a hydrophobic Ile residue instead of a hydrophilic Thr residue, resulted in a large decrease in ENR enzymatic activity.

A Deficiency in ENR Leads to a Decrease in Total Lipid Content in *mod1* Plants

In plant cells, almost all the fatty acids are found to be esterified or otherwise modified into lipid forms, such as glycerolipids, triacylglycerol, and cuticular lipids (Topfer et al., 1995). To determine whether fatty acid biosynthesis was affected in *mod1* plants, we extracted total lipids from wild-type and *mod1* plants grown at 20 or 26°C. The total lipid contents of the *mod1* plants grown at 20 or 26°C were 9 and

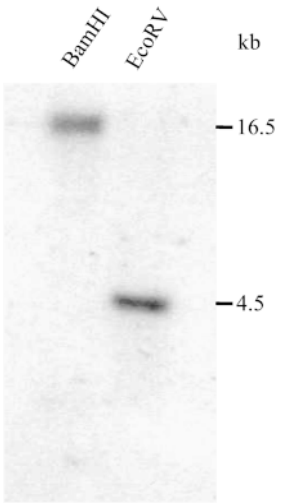

Figure 7. DNA Gel Blot Analysis.

Arabidopsis Col-0 DNA was digested separately with BamHI and EcoRV and transferred onto a Hybond N^+ membrane. The filter was probed with an *ENR* gene fragment. Lengths of DNA fragments in kilobases are indicated at right.

12% lower, respectively, than those of the wild type (Figure 9). These results indicate that the *mod1* mutation does indeed affect fatty acid biosynthesis, which in turn causes a reduction in total lipid content.

DISCUSSION

It has long been recognized that cell death is required in plant growth and development. Recent studies have found that plant cell death often has some of the characteristics of apoptosis described for animal cells, such as condensation and shrinkage of the cytoplasm and nucleus and fragmentation of the nuclear DNA (Greenberg, 1996). Despite these similarities between cell death in plants and animals, it is unclear whether cell death is mediated by the same mechanisms in both kingdoms (Pennell and Lamb, 1997). To understand the process of cell death in plants, we took a genetic approach in screening for cell death mutants in Arabidopsis and isolated a novel premature cell death mutant, *mod1*. We have systematically characterized this mutant and cloned the gene responsible for the mutant phenotype. The *MOD1* gene encodes an ENR that catalyzes the last reduction step in the de novo fatty acid biosynthesis cycle. A single amino acid substitution in *mod1* ENR causes a marked decrease in ENR activity, which leads to a reduction of ~10% in total lipid content in *mod1* plants and severe morphological phenotypes.

The de novo fatty acid biosynthesis pathway is one of the most important primary metabolic pathways in all cellular organisms, generating the palmitic and stearic acids that serve as the precursors for other fatty acids of different lengths and saturation levels. In plant cells, most fatty acids are found in lipid forms, such as diacylglycerol, sphingomyelin, and ceramide, which function either as essential components of cell membranes or as important regulators of cell growth and differentiation (Ohlrogge and Browse, 1995; Topfer et al., 1995; Okazaki et al., 1998). Therefore, a null mutation that completely blocks de novo fatty acid biosynthesis would almost certainly be lethal. Even though ENR activity in *mod1* plants is barely detectable, the mutant still accumulates ~90% of the total lipid content of wild-type plants. This suggests that the in vivo activity of ENR is in excess in wild-type plants to the extent that its residual activity in *mod1* is able to support the minimal biosynthesis of fatty acids required for *mod1* growth.

The reduction in total lipid content in *mod1* plants is consistent with data for the bacterial temperature-sensitive mutant *envM*, which is also deficient in ENR activity (Bergler et al., 1994). When *envM* mutant plants were shifted to a nonpermissive high temperature, fatty acid and phospholipid

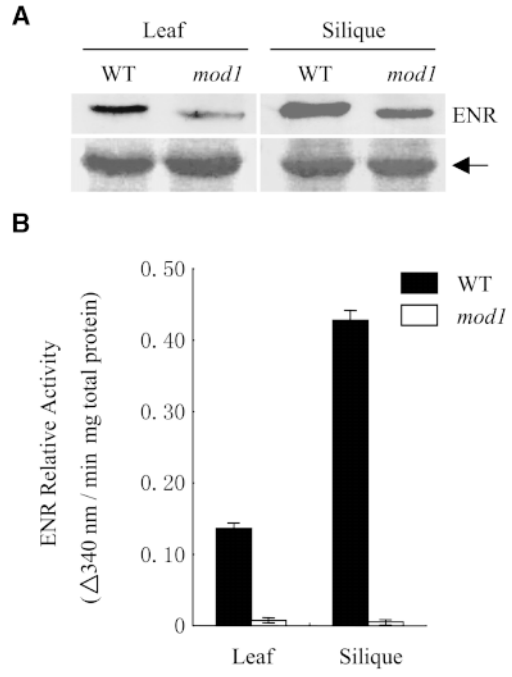

Figure 8. ENR Protein Content and Its Enzymatic Activity in *mod1* and Wild-Type Plants.

(A) Protein gel blot analysis. Protein samples prepared from *mod1* and wild-type (WT) plants 30 days after imbibition and from siliques 15 days after flowering were analyzed by immunoblotting. The arrow indicates the nonspecific protein, which served as a loading control.
(B) ENR activity in Arabidopsis leaves and siliques. Samples were prepared from the leaves and siliques of *mod1* and wild-type (WT) plants. ENR activity is shown as mean ±SE ($n = 3$).

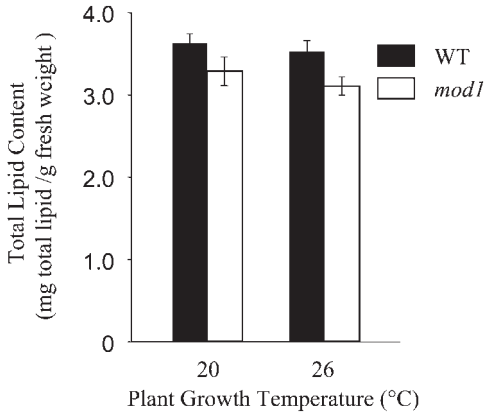

Figure 9. Comparison of Total Lipid Contents between *mod1* and Wild-Type Plants.

Total lipid content was determined in 10-g samples of fresh rosette leaves from 4-week-old plants. The total lipid contents are shown as mean ±SE ($n = 2$).

biosynthesis were profoundly inhibited (Bergler et al., 1992; Kater et al., 1994). Like the bacterial *envM* mutant, the Arabidopsis *mod1* mutant is also sensitive to temperature. The morphological abnormalities of *mod1* plants are much more severe at 26 than at 20°C (Figure 5). Because no differences in ENR activities were detected between the high and low temperatures (data not shown), the temperature sensitivity of *mod1* plants may not originate from the temperature sensitivity of ENR itself but rather from abnormal cell membranes, the result of deficiencies in fatty acids.

Impairment of fatty acid biosynthesis interferes with the integration of cell membranes. When bacterial cells in early logarithmic phase were treated with diazaborine, an inhibitor of fatty acid synthesis that targets ENR, the majority of the rod-shaped cells showed zones of enhanced transparency at the poles, the result of retraction of the inner membrane (Turnowsky et al., 1989). A similar morphological alteration was observed when *envM* mutant bacteria were cultured under nonpermissive conditions (Turnowsky et al., 1989). In both cases, the shrunken cell phenotypes resulted from insufficient fatty acid synthesis by way of inhibition of the ENR activities. In *mod1*, which also bears a defective ENR, the chloroplast thylakoid membrane in the chlorotic sectors was severely disorganized, suggesting that the cell membrane system may also be affected to some degree. This might explain why mesophyll cells in *mod1* chlorotic sectors are irregular in size and shape (Figure 2). Furthermore, the different sizes and shapes of *mod1* cells are indicative of uneven cell growth and expansion, which we believe progressively causes the curling of leaves and siliques.

Lipids are major building blocks of cell membrane. Cells in young tissues need a sufficient supply of these basic building materials for vigorous growth or division. The high expression of *ENR* seen in young leaves and shoot and root meristems (Ohlrogge and Jaworski, 1997) may explain why the chlorotic phenotype always appears in young tissues in *mod1*, such as newly emerging leaves, inflorescences, and siliques. However, the chlorotic phenotype does not appear in *mod1* seedlings; at this stage, fatty acid synthesis must still be sufficient to support slow growth.

Interruption of a vital metabolic process inevitably leads to cell death (Vaux and Korsmeyer, 1999). In human cancer cells, fatty acid synthetic metabolism is abnormally increased. Inhibition of FAS in tumor cells induces apoptosis by producing rapid and profound inhibition of DNA replication and S phase progression (Pizer et al., 1998). In *mod1* plants, impairment of fatty acid biosynthesis resulting from deficiency of ENR will also induce cell death; however, only a few cells actually die. The mosaic death pattern might be explained as follows. In *mod1* plants, the deficiency in ENR leads to reduction in fatty acid biosynthesis, which in turn affects the integration of cell membranes. As a result, some cells become more vulnerable and start the death process, which might then release some signals to induce their surrounding cells to undergo cell death and form the morphologically defective clusters (Figures 3E to 3H).

Although condensed cytoplasm and a DNA ladder were observed, we are not certain whether cell death in *mod1* plants is an active apoptotic process. In cellular organisms, fatty acids function in constructing the cell membrane and regulating cell proliferation, differentiation, and apoptosis (Okazaki et al., 1998). According to our current understanding and classification, cell death originating from the lack of an essential compound is thought to be nonphysiological (Vaux and Korsmeyer, 1999). However, physiological cell death (apoptosis) induced or inhibited by lipids such as sphingomyelin, ceramide, and diacylglycerol has been well established in animal cells (Jarvis et al., 1994; Dawson et al., 1998). Therefore, the cell death observed in *mod1* plants may result from the lack of essential compounds, the alteration of signaling molecules, or both. Further investigation is needed to address this important question.

Plant cell death resulting from the impairment of metabolic pathways has been described in tobacco and maize. Overexpression of the transcription factor AmMYB308 in transgenic tobacco inhibits the metabolism of phenolic acid, leading to a deficiency in antioxidants of phenolic acid esters and a subsequent increase in the concentration of reactive oxygen species that trigger cell death (Tamagnone et al., 1998). In the maize mutant *Les22*, impairment of the porphyrin biosynthesis pathway results in accumulation of uroporphyrin, which induces the production of cell-damaging oxygen free radicals (Hu et al., 1998). In both cases, cell death is actually caused by the toxic compounds generated by the altered metabolic pathways.

The Arabidopsis *mod1* mutant represents a new class of cell death mutants that are deficient in fatty acid synthesis. Investigation of *mod1* plants will allow us to gain insight into the signal transduction of cell death resulting from the

impairment of a primary metabolic pathway (Vaux and Korsmeyer, 1999). The temperature sensitivity of the *mod1* mutant is also useful in identifying genes whose expression is regulated when the stress of high temperature is applied. In addition, the *mod1* mutant can be used in elucidating regulatory mechanisms of the de novo fatty acid biosynthetic pathway in plants.

METHODS

Plant Growth

Plants (*Arabidopsis thaliana*) were grown basically on vermiculite saturated with 0.3 × B_5 medium under continuous illumination (80 to 120 μE m^{-2} sec^{-1}) at 23°C, as described previously (Li et al., 1993), or under the conditions specified in the text. For treatment with high temperature (26°C), plants were geminated and grown at normal temperature (23°C) for 10 days after imbibition and then transferred into a high-temperature growth room. For assessing the effects of plant hormones or nutrients, plants were grown on PNS medium (Haughn and Somerville, 1986) containing the tested supplement as indicated.

Mutant Screening

The *mod1* mutant was identified by growing M_2 seeds on vermiculite under continuous light at 23°C. M_2 seeds in the Columbia (Col-0) genetic background were obtained by mutagenesis with ethyl methanesulfonate, as described by Barczak et al. (1995). Putative programmed cell death (PCD) mutants were identified by examining for chlorotic morphology after 4 weeks of growth and then allowed to self-pollinate. The phenotype of M_3, F_1, or F_2 seeds was confirmed under the growth conditions described above.

Histochemistry and Microscopy

Four-week-old leaves were fixed in formalin–glacial acetic acid–70% ethanol (1:1:18) for 48 hr and transferred into 70% ethanol. Samples were rinsed in 50% ethanol and then distilled water and were directly mounted for the observation of mesophyll cells under a differential interference contrast microscope (model BH-2; Olympus, Tokyo, Japan). For chloroplast observations, samples were stained with 0.1% safranin O for 10 min, rinsed with distilled water, and hydrolyzed with 0.1 M HCl in a 50°C water bath for 20 min. The hydrolyzed samples were then mounted and observed under a light microscope (model BH-2; Olympus). Trypan blue staining was performed as previously described (Keogh et al., 1980; Bowling et al., 1997; Peterhänsel et al., 1997). Samples were covered with an alcoholic lactophenol trypan blue mixture (30 mL of ethanol, 10 g of phenol, 10 mL of water, 10 mL of glycerol, 10 mL of lactic acid, and 10 mg of trypan blue), placed in a boiling water bath for 2 to 3 min, and then left at room temperature for 1 hr. The samples were transferred into a chloral hydrate solution (2.5 g mL^{-1}) and boiled for 20 min to destain. After multiple exchanges of chloral hydrate solution to reduce the background, samples were equilibrated with 50% glycerol, mounted, and observed with a stereomicroscope (model SZX-12; Olympus).

Chlorophyll Fluorescence and Chlorophyll Quantification

To observe UV-induced chlorophyll fluorescence, we peeled away the epidermis of fresh leaves and observed the mesophyll under long-wavelength (365 nm) UV light with a fluorescence microscope (model BX-60; Olympus). Chlorophyll concentrations were calculated from the absorbance at 646 and 663 nm in an 80% (v/v) acetone extract, as described by Lichtenthaler (1987).

Electron Microscopy

Samples were prepared as described by Dörmann et al. (1995) and Itoh et al. (1998), with some modifications. Briefly, rosette leaves of 3- to 4-week-old plants were fixed with 4% (v/v) glutaraldehyde in 0.1 M sodium phosphate buffer, pH 7.2, and incubated at 4°C overnight. After being rinsed with 0.1 M sodium phosphate buffer, pH 7.2, they were postfixed in 1% (w/v) osmium tetroxide for 2 hr at 4°C and rinsed with the same buffer. Samples were then dehydrated in a graded series of ethanol. For scanning electron microscopy, 100% ethanol was replaced with 3-methylbutyl acetate. Samples were critical-point dried, sputter-coated with platinum, and observed under a scanning electron microscope (model S-570; Hitachi, Tokyo, Japan). For transmission electron microscopy, samples were embedded in Spurr's epoxy resin. Ultrathin sections (70 nm) were stained with uranyl acetate and viewed in a transmission electron microscope (model EM-200; Hitachi).

DNA Gel Blot Analysis

Total Arabidopsis DNA isolated from 4-week-old plants was prepared as previously described (Li et al., 1995). For gel blot analysis of DNA fragmentation, equal amounts of DNA from *mod1* or wild-type plants were separated by 2% agarose gel electrophoresis immediately after isolation. The DNA was then transferred onto a Hybond N^+ membrane (Amersham) and hybridized with a ^{32}P-labeled Sau3AI-digested genomic DNA probe. For analysis of the *ENR* gene copy number in Arabidopsis, genomic DNA was completely digested with BamHI and EcoRV and then separated in a 0.8% agarose gel. DNA was transferred onto a Hybond N^+ filter. Blots were prehybridized at 65°C in prehybridization solution (6 × SSC [1 × SSC is 0.15 M NaCl and 0.015 M sodium citrate], 0.5% SDS, 100 μg mL^{-1} denatured salmon sperm DNA, and 5 × Denhardt's solution [1 × Denhardt's solution is 0.02% Ficoll, 0.02% polyvinylpyrrolidone, and 0.02% BSA]) for 3 hr and hybridized at 65°C in prehybridization solution containing ^{32}P-labeled *ENR* fragment DNA probes. Blots were then washed under low-stringency conditions (5 min in 2 × SSC and 0.1% SDS at room temperature and 10 min in 1 × SSC and 0.1% SDS at room temperature).

Genetic Analysis and Primary Mapping of the *mod1* Locus

Homozygous mosaic death *mod1* plants generated from three rounds of backcrosses with wild-type Col-0 were used in standard genetic analysis and mapping, as previously described (Li and Last,

1996). The phenotype of the *mod1* mutant was scored after 3 to 4 weeks of growth under continuous light at 23°C. An F_2 mapping population was generated from crosses between *mod1* (in the Col-0 background) and the polymorphic Landsberg *erecta* (L*er*) ecotype. The F_1 progeny were allowed to self-pollinate, and the F_2 plants were scored for chlorosis and curled leaves. DNA was prepared from the parental, F1, and 822 F2 mutant progeny. The genetic linkage between mod1 and molecular markers was determined by using codominant polymerase chain reaction–based cleaved amplified polymorphic sequences (CAPS) markers (Konieczny and Ausubel, 1993) or microsatellite markers (Bell and Ecker, 1994), and analyzed with Mapmaker (Lander et al., 1987). The restriction fragment length polymorphism marker mi421 was converted into a CAPS marker by sequencing the clone and designing primers based on its sequence. After determining that mod1 lay between IGS1 and mi421, we used these two CAPS markers to identify recombinants from 2014 F_2 mapping plants, obtaining 54 and 14 recombinants, respectively.

Fine Mapping of the *mod1* Locus

Yeast artificial chromosome (YAC) clones covering the interval between *IGS1* and mi412 (Zachgo et al., 1996) were used to isolate their ends (CIC9A3R, CIC11C7L, and CIC2G5R) through inverse polymerase chain reaction or plasmid rescue, as described previously (Gibson and Somerville, 1992). The three YAC ends and a restriction fragment length polymorphism marker CDs3 were sequenced to test polymorphisms between Col-0 and L*er*. Only CIC9A3R was converted into a CAPS marker. Linkage analysis placed the *mod1* locus between CIC9A3R and mi421. We then screened the TAMU bacterial artificial chromosome (BAC) library (Choi et al., 1995), using CIC9A3R, CIC11C7L, CIC2G5R, and CDs3 as probes, and identified 31 BAC clones. A contig consisting of TAMU6P5, TAMU7M23, TAMU12A21, and TAMU18A18 was constructed (Mou et al., 2000). Four new CAPS markers (TAMU6P5-4.8, TAMU18A18E1, TAMU18A18E2, and TAMU12A21E1) were developed, and the *mod1* locus was narrowed down to the interval between TAMU6P5-4.8 and CIC9A3R. Both markers were used to isolate genomic clones from a phage library (Col-0). The DNA fragments of CAPS markers were amplified under the following conditions: denaturation at 94°C for 3 min, 45 cycles (94°C for 1 min, 56°C for 1 min, and 72°C for 2 min), and final extension at 72°C for 10 min. The detailed information of all the newly developed CAPS markers has been deposited in the Arabidopsis public database.

Complementation of *mod1*

A T-DNA binary vector was derived from pBI101 (Clontech, Palo Alto, CA) as follows. The pBI101 vector was digested with SmaI and EcoRI, blunted with the Klenow fragment of DNA polymerase I, and self-ligated to form a new binary vector, pJL482. A 7.0-kb BamHI genomic DNA fragment (Figure 6C) was ligated to pJL482, forming pJL635, which contains the entire *ENR* gene and sufficient *cis* elements. Meanwhile, a 6.5-kb genomic DNA containing a partial *ENR* gene and 5′ upstream sequence was inserted into pJL482, generating pJL656. Both pJL635 and pJL656 were introduced into the Agrobacterium strain GV3101(pMP90) by electroporation and were used to transform *mod1* plants by means of vacuum infiltration (Bechtold et al., 1993). The phenotype of the *mod1* mutant was scored in T_1 transformants and T_2 progeny.

Protein Gel Blot Analysis

The MfeI (blunt-ended)-EcoRI fragment of the full-length *ENR* cDNA (pJL659) was cloned into the SmaI-EcoRI–digested *Escherichia coli* expression vector pGEX2T (Pharmacia) and then introduced into *E. coli* by electroporation. The expression and purification of the fusion protein, antibody preparation, and immunological detection were conducted as previously described (Liu et al., 1999). Protein was extracted from Arabidopsis leaves and siliques as described by Fawcett et al. (1994), aliquoted into 50-μL lots, and stored at −80°C.

ENR Activity Assay and Total Lipid Determination

ENR activity was measured by monitoring the decrease in absorbance at 340 nm, as described by Slabas et al. (1986). Protein content was measured with the Bio-Rad protein assay kit, and 50 μg of protein was used for each ENR activity assay. Total lipid content was determined by using the Soxhlet extraction method (Zhong, 1985). Briefly, 10 g of fresh rosette leaves of 4-week-old plants was dried at 80°C for 4 hr and ground into powder with a mortar. The powder was completely extracted with ether in a Soxhlet apparatus in a 70 to 80°C waterbath for 8 to 10 hr.

ACKNOWLEDGMENTS

We thank David Stern, Xinnian Dong, and Daowen Wang for comments on the manuscript, Jian Ouyang for technical assistance in computer-generated graphics, and Guangjun Dong for assistance with electron microscopy. Gifts of Arabidopsis M_2 seeds from Robert L. Last (Cereon Genomics LLP, Cambridge, MA), CDs3 DNA clone from Georges Picard (University of Blaise Pascal, Aubière, France), and GV3101(pMP90) from Stanton B. Gelvin (Purdue University, West Lafayette, IN) are much appreciated. The TAMU BAC library filters and the clones (BAC, YAC, and mi421 plasmid) were provided by the Arabidopsis Biological Resource Center (Ohio State University, Columbus). This research was supported by grants from the National Natural Science Foundation of China and the High Technology Program and a National Distinguished Young Scholar Award to J.L.

Received October 12, 1999; accepted January 10, 2000.

REFERENCES

Barczak, A.J., Zhao, J., Pruitt, K.D., and Last, R.L. (1995). 5-Fluoroindole resistance identifies tryptophan synthase beta subunit mutants in *Arabidopsis thaliana.* Genetics **140**, 303–313.

Bechtold, N., Ellis, J., and Pelletier, G. (1993). In planta *Agrobacterium*–mediated gene transfer by infiltration of adult *Arabidopsis thaliana* plants. C.R. Acad. Sci. Ser. III Sci. Vie **316,** 1194–1199.

Bell, C.J., and Ecker, J.R. (1994). Assignment of 30 microsatellite loci to the linkage map of Arabidopsis. Genomics **19,** 137–144.

Bergler, H., Hogenauer, G., and Turnowsky, F. (1992). Sequences

of the *envM* gene and of two mutated alleles in *Escherichia coli.* J. Gen. Microbiol. **138,** 2093–2100.

Bergler, H., Wallner, P., Ebeling, A., Leitinger, B., Fuchsbichler, S., Aschauer, H., Kollenz, G., Hogenauer, G., and Turnowsky, F. (1994). Protein EnvM is the NADH-dependent enoyl-ACP reductase (FabI) of *Escherichia coli.* J. Biol. Chem. **269,** 5493–5496.

Bleecker, A.B., and Patterson, S.E. (1997). Last exit: Senescence, abscission, and meristem arrest in Arabidopsis. Plant Cell **9,** 1169–1179.

Botella, M.A., Parker, J.E., Frost, L.N., Bittner-Eddy, P.D., Beynon, J.L., Daniels, M.J., Holub, E.B., and Jones, J.D. (1998). Three genes of the Arabidopsis *RPP1* complex resistance locus recognize distinct *Peronospora parasitica* avirulence determinants. Plant Cell **10,** 1847–1860.

Bowling, S.A., Clarke, J.D., Liu, Y., Klessig, D.F., and Dong, X. (1997). The *cpr5* mutant of Arabidopsis expresses both NPR1-dependent and NPR1-independent resistance. Plant Cell **9,** 1573–1584.

Bush, D.S., Biswas, A.K., and Jones, R.L. (1989). Gibberellic acid–stimulated Ca^{2+} accumulation in endoplasmic reticulum of barley aleurone: Ca^{2+} transport and steady-state levels. Planta **178,** 411–420.

Choi, S., Creelman, R.A., Mullet, J.E., and Wing, R.E. (1995). Construction and characterization of a bacterial artificial chromosome library of *Arabidopsis thaliana.* Plant Mol. Biol. Rep. **13,** 124–128.

Cohen, J.J. (1993). Apoptosis. Immunol. Today **14,** 126–130.

Dangl, J.L., Dietrich, R.A., and Richberg, M.H. (1996). Death don't have no mercy: Cell death programs in plant–microbe interactions. Plant Cell **8,** 1793–1807.

Dawson, G., Goswami, R., Kilkus, J., Wiesner, D., and Dawson, S. (1998). The formation of ceramide from sphingomyelin is associated with cellular apoptosis. Acta Biochim. Pol. **45,** 287–297.

Dietrich, R.A., Delaney, T.P., Uknes, S.J., Ward, E.R., Ryals, J.A., and Dangl, J.L. (1994). Arabidopsis mutants simulating disease resistance response. Cell **77,** 565–577.

Dietrich, R.A., Richberg, M.H., Schmidt, R., Dean, C., and Dangl, J.L. (1997). A novel zinc finger protein is encoded by the Arabidopsis *LSD1* gene and functions as a negative regulator of plant cell death. Cell **88,** 685–694.

Dörmann, P., Hoffmann-Benning, S., Balbo, I., and Benning, C. (1995). Isolation and characterization of an Arabidopsis mutant deficient in the thylakoid lipid digalactosyl diacylglycerol. Plant Cell **7,** 1801–1810.

Egan, A.F., and Russell, R.R.B. (1973). Conditional mutations affecting the cell envelope of *Escherichia coli* K-12. Genet. Res. **21,** 139–152.

Farmer, E.D., Weber, H., and Vollenweider, S. (1998). Fatty acid signaling in *Arabidopsis.* Planta **206,** 167–174.

Fawcett, T., Simon, W.J., Swinhoe, R., Shanklin, J., Nishida, I., Christie, W.W., and Slabas, A.R. (1994). Expression of mRNA and steady-state levels of protein isoforms of enoyl-ACP reductase from *Brassica napus.* Plant Mol. Biol. **26,** 155–163.

Fukuda, H. (1997). Tracheary element differentiation. Plant Cell **9,** 1147–1156.

Gibson, S.I., and Somerville, C.R. (1992). Chromosome walking in *Arabidopsis thaliana* using yeast artificial chromosomes. In Methods in Arabidopsis Research, C. Koncz, N.-H. Chua, and J. Schell, eds (Singapore: World Scientific), pp. 119–143.

Gray, J., Close, P.S., Briggs, S.P., and Johal, G.S. (1997). A novel suppressor of cell death in plants encoded by the *Lls1* gene of maize. Cell **89,** 25–31.

Greenberg, J.T. (1996). Programmed cell death: A way of life for plants. Proc. Natl. Acad. Sci. USA **93,** 12094–12097.

Greenberg, J.T., Guo, A., Klessig, D.F., and Ausubel, F.M. (1994). Programmed cell death in plants: A pathogen-triggered response activated coordinately with multiple defense functions. Cell **77,** 551–563.

Haughn, G.W., and Somerville, C. (1986). Sulfonylurea-resistant mutants of *Arabidopsis thaliana.* Mol. Gen. Genet. **204,** 430–434.

Hu, G., Yalpani, N., Briggs, S.P., and Johal, G.S. (1998). A porphyrin pathway impairment is responsible for the phenotype of a dominant disease lesion mimic mutant of maize. Plant Cell **10,** 1095–1105.

Itoh, J.I., Hasegawa, A., Kitano, H., and Nagato, Y. (1998). A recessive heterochronic mutation, plastochron1, shortens the plastochron and elongates the vegetative phase in rice. Plant Cell **10,** 1511–1522.

Jarvis, W.D., Kolesnick, R.N., Fornari, F.A., Traylor, R.S., Gewirtz, D.A., and Grant, S. (1994). Induction of apoptotic DNA damage and cell death by activation of the sphingomyelin pathway. Proc. Natl. Acad. Sci. USA **91,** 73–77.

Kamoun, S., van West, P., Vleeshouwers, V.G., de Groot, K.E., and Govers, F. (1998). Resistance of *Nicotiana benthamiana* to *Phytophthora infestans* is mediated by the recognition of the elicitor protein INF1. Plant Cell **10,** 1413–1426.

Kater, M.M., Koningstein, G.M., Nijkamp, H.J., and Stuitje, A.R. (1991). cDNA cloning and expression of *Brassica napus* enoyl-acyl carrier protein reductase in *Escherichia coli.* Plant Mol. Biol. **17,** 895–909.

Kater, M.M., Koningstein, G.M., Nijkamp, H.J., and Stuitje, A.R. (1994). The use of a hybrid genetic system to study the functional relationship between prokaryotic and plant multi-enzyme fatty acid synthetase complexes. Plant Mol. Biol. **25,** 771–790.

Keogh, R.C., Deberall, B.J., and McLeod, S. (1980). Comparison of histological and physiological responses to *Phakospora pachyrhizi* in resistant and susceptible soybean. Trans. Br. Mycol. Soc. **74,** 329–333.

Konieczny, A., and Ausubel, F.M. (1993). A procedure for mapping Arabidopsis mutations using co-dominant ecotype-specific PCR-based markers. Plant J. **4,** 403–410.

Kuo, A., Cappelluti, S., Cervantes-Cervantes, M., Rodriguez, M., and Bush, D.S. (1996). Okadaic acid, a protein phosphatase inhibitor, blocks calcium changes, gene expression, and cell death induced by gibberellin in wheat aleurone cells. Plant Cell **8,** 259–269.

Lander, E.S., Green, P., Abrahamson, J., Barlow, A., Daly, M.J., Lincoln, S.E., and Newberg, L. (1987). Mapmaker: An interactive computer package for constructing primary genetic linkage maps of experimental and natural populations. Genomics **1,** 174–181.

Li, J., and Last, R.L. (1996). The *Arabidopsis thaliana trp5* mutant has a feedback-resistant anthranilate synthase and elevated soluble tryptophan. Plant Physiol. **110,** 51–59.

Li, J., Ou-Lee, T.-M., Raba, R., Amundson, R.G., and Last, R.L. (1993). Arabidopsis flavonoid mutants are hypersensitive to UV-B irradiation. Plant Cell **5,** 171–179.

Li, J., Zhao, J., Rose, A.B., Schmidt, R., and Last, R.L. (1995). Arabidopsis phosphoribosyl-anthranilate isomerase: Molecular genetic analysis of triplicate tryptophan pathway genes. Plant Cell **7,** 447–461.

Lichtenthaler, H.K. (1987). Chlorophylls and carotenoids: Pigments of photosynthetic biomembranes. Methods Enzymol. **148,** 350–382.

Liu, X., Ouyang, J., He, Y., and Li, J. (1999). Immunological analysis of Arabidopsis indole-3-glycerol phosphate synthase. Acta Bot. Sin. **41,** 751–756.

Marchetti, M.A., Bollich, C.N., and Uecker, F.A. (1983). Spontaneous occurrence of the Sekiguchi lesion in two American rice lines: Its induction, inheritance, and utilization. Phytopathology **73,** 603–606.

McDowell, J.M., Dhandaydham, M., Long, T.A., Aarts, M.G., Goff, S., Holub, E.B., and Dangl, J.L. (1998). Intragenic recombination and diversifying selection contribute to the evolution of downy mildew resistance at the *RPP8* locus of Arabidopsis. Plant Cell **10,** 1861–1874.

Mou, Z., Dai, Y., and Li, J. (2000). Fine-mapping of an Arabidopsis cell death mutation locus. Sci. China **43,** 138–145.

Ohlrogge, J., and Browse, J. (1995). Lipid biosynthesis. Plant Cell **7,** 957–970.

Ohlrogge, J.B., and Jaworski, J.G. (1997). Regulation of fatty acid synthesis. Annu. Rev. Plant Physiol. Plant Mol. Biol. **48,** 109–136.

Okazaki, T., Kondo, T., Kitano, T., and Tashima, M. (1998). Diversity and complexity of ceramide signaling in apoptosis. Cell Signal **10,** 685–692.

Pennell, R.I., and Lamb, C. (1997). Programmed cell death in plants. Plant Cell **9,** 1157–1168.

Peterhänsel, C., Freialdenhoven, A., Kurth, J., Kolsch, R., and Schulze-Lefert, P. (1997). Interaction analyses of genes required for resistance responses to powdery mildew in barley reveal distinct pathways leading to leaf cell death. Plant Cell **9,** 1397–1409.

Pizer, E.S., Chrest, F.J., DiGiuseppe, J.A., and Han, W.F. (1998). Pharmacological inhibitors of mammalian fatty acid synthase suppress DNA replication and induce apoptosis in tumor cell lines. Cancer Res. **58,** 4611–4615.

Roggenkamp, R., Numa, S., and Schweizer, E. (1980). Fatty acid–requiring mutant of *Saccharomyces cerevisiae* defective in acetyl-CoA carboxylase. Proc. Natl. Acad. Sci. USA **77,** 1814–1817.

Slabas, A.R., and Fawcett, T. (1992). The biochemistry and molecular biology of plant lipid biosynthesis. Plant Mol. Biol. **19,** 169–191.

Slabas, A.R., Sidebottom, C.M., Hellyer, A., Kessell, R.M.J., and Tombs, M.P. (1986). Induction, purification and characterization of NADH-specific enoyl acyl carrier protein reductase from developing seeds of oil seed rape (*Brassica napus*). Biochim. Biophys. Acta **877,** 271–280.

Somerville, C., and Browse, J. (1991). Plant lipids: Metabolism, mutants, and membranes. Science **252,** 80–87.

Stuitje, A., Kater, M.M., Verwoert, I.I.G.S., Fawcett, T., Slabas, A.R., and Nijkamp, H.J.J. (1993). Molecular genetic studies of plant enoyl-ACP reductase and bacterial malonyl CoA-ACP transacylase genes. In Biochemistry and Molecular Biology of Membrane and Storage Lipids of Plants, N. Murata and C. Somerville, eds (Rockville, MD: American Society of Plant Physiologists), pp. 121–132.

Tamagnone, L., Merida, A., Stacey, N., Plaskitt, K., Parr, A., Chang, C.F., Lynn, D., Dow, J.M., Roberts, K., and Martin, C. (1998). Inhibition of phenolic acid metabolism results in precocious cell death and altered cell morphology in leaves of transgenic tobacco plants. Plant Cell **10,** 1801–1816.

Topfer, R., Martini, N., and Schell, J. (1995). Modification of plant lipid synthesis. Science **268,** 681–686.

Turnowsky, F., Fuchs, K., Jeschek, C., and Hogenauer, G. (1989). *envM* genes of *Salmonella typhimurium* and *Escherichia coli.* J. Bacteriol. **171,** 6555–6565.

Vaux, D.L., and Korsmeyer, S.J. (1999). Cell death in development. Cell **96,** 245–254.

Wang, M., Oppedijk, B.J., Lu, X., Van Duijn, B., and Schilperoort, R.A. (1996). Apoptosis in barley aleurone during germination and its inhibition by abscisic acid. Plant Mol. Biol. **32,** 1125–1134.

Wolter, M., Hollricher, K., Salamini, F., and Schulze-Lefert, P. (1993). The *mlo* resistance alleles to powdery mildew infection in barley trigger a developmentally controlled defence mimic phenotype. Mol. Gen. Genet. **239,** 122–128.

Wyllie, A.H., Kerr, J.F.R., and Currie, A.R. (1980). Cell death: The significance of apoptosis. Int. Rev. Cytol. **68,** 251–306.

Yeung, E.C., and Meinke, D.W. (1993). Embryogenesis in angiosperms: Development of the suspensor. Plant Cell **5,** 1371–1381.

Zachgo, E.A., Wang, M.L., Dewdney, J., Bouchez, D., Camilleri, C., Belmonte, S., Huang, L., Dolan, M., and Goodman, H.M. (1996). A physical map of chromosome 2 of *Arabidopsis thaliana.* Genome Res. **6,** 19–25.

Zhong, W. (1985). Determination of the total lipids in plants. In Laboratory Manual of Plant Physiology, Y. Xue and Z. Xia, eds (Shanghai, China: Shanghai Science and Technology Press), pp. 198–201.